ChemComm

FEATURE ARTICLE

View Article Online
View Journal | View Issue

Cite this: *Chem. Commun.*, 2020, **56**, 1767

Design and application of aminoacridinium organophotoredox catalysts

Bouthayna Zilate, Christian Fischer and Christof Sparr *

Received 31st October 2019,
Accepted 16th January 2020

DOI: 10.1039/c9cc08524f

rsc.li/chemcomm

Recent developments in preparative photocatalysis have reshaped synthetic strategies and now represent an integral part of current organic chemistry. Due to their favourable electrochemical and photophysical properties, the nowadays most frequently used photocatalysts are based on precious Ru- and Ir-polypyridyl complexes. Apart from that, organic catalysts such as the acridinium salts are now commonly employed to complement transition metals to provide potentially sustainable strategies amenable to large-scale synthesis. In this feature article, the design, synthesis and application of aminoacridinium photoredox catalysts as well as their exceptionally broad range of redox properties are highlighted. Due to their modularity, this burgeoning class of organophotocatalysts is anticipated to contribute significantly to synthetic methodology development and the translation to a wide range of innovative implementations.

1. Introduction

Polypyridyl transition metal systems have been transformative for the field of photoredox catalysis with ruthenium and iridium catalysts representing particularly versatile scaffolds (Scheme 1).[1–4] The wide range of properties due to the tunability of their ligands make them exceptionally valuable catalysts for photochemical transformations. With the development of fully organic alternatives, the area opened up towards potentially sustainable processes.[5–7] Among them, acridinium salts pioneered by Fukuzumi[8,9] are known to have remarkable photophysical properties, complementary to those of polypyridyl transition metal structures. Their high reduction potential in the excited state (often $E_{1/2}$ $[P^*/P^-] > 2$ V *vs.* SCE) and their robustness, pH independence, and high solubility in a variety of solvents, render them valuable photocatalysts for a wide range of preparative transformations.

Department of Chemistry, University of Basel, St. Johanns-Ring 19, CH-4056, Basel, Switzerland. E-mail: christof.sparr@unibas.ch

2. Design and synthesis of acridinium salts

The design of acridinium dyes initially evolved towards an increased chemical stability. First, Fukuzumi integrated a bulky mesityl group at the C9 position to prevent nucleophilic

Bouthayna Zilate

Bouthayna Zilate was born in 1988 in Casablanca (Morocco), studied pharmacy at the University of Paris V where she obtained her MSc with Prof. Hervé Galons working on inhibitors of cyclin-dependent kinases (CDK). In 2016, she started a PhD in the group of Prof. Sparr at the University of Basel. She's currently investigating novel approaches for the synthesis of acridinium salts and their application in photoredox catalysis.

Christian Fischer

Christian Fischer grew up in Bern and studied chemistry at the University of Basel. He worked with Prof. Oliver S. Wenger and Prof. Karl Gademann and completed his Master's thesis in the group of Prof. Christof Sparr. In his PhD studies he focused on the development of new, sustainable methods and catalysts. In December 2018, he joined the research group of Prof. Dirk Trauner (New York University) as an SNSF postdoctoral fellow, to investigate the photopharmacological control of biological processes.

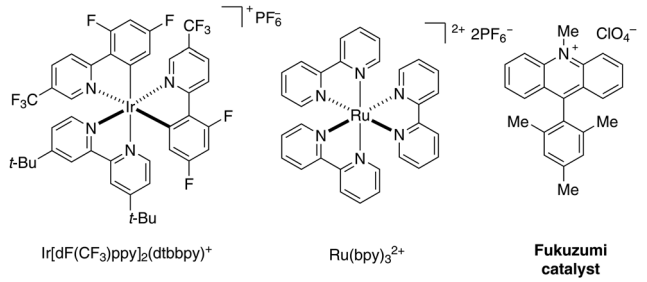

Scheme 1 Selection of commonly used photoredox catalysts.

addition that results in photobleaching.[8] Moreover, the introduction of electron donating groups favours charge transfer by the stabilizing mesityl moiety.[10] As a consequence, the Mes-Me-Acr$^+$ displays unique oxidizing properties ($E_{1/2}$ [P^*/P^-] = +2.08 V *vs.* SCE), with a suitable lifetime of the singlet and triplet excited state, which renders it a valuable catalyst for numerous photochemical reactions.[11–14]

To further overcome competitive dealkylation processes, Nicewicz developed *N*-arylated acridinium salts with higher chemical stability and an extended range of redox properties ($E_{1/2}$ [P^*/P^-] = 1.62–2.08 V *vs.* SCE, Scheme 2).[15] A series of symmetrically substituted acridinium salts were prepared, with alkyl or methoxy substituents attached to the acridinium core.

A one step synthesis featuring a triarylamine precursor in a Friedel–Crafts reaction with a benzoyl chloride derivative delivered the desired acridinium salt **6** with a tetrasubstituted core in good yields (71–81%, Scheme 3). The construction of other acridinium salts with a disubstituted core proved to be more challenging, requiring several steps including an addition of a Grignard reagent to an acridone. For a modular synthesis of acridinium salts (7, X = N) and other heterocyclic analogues such as xanthylium dyes (7, X = O), we thus investigated the use of 1,5-bifunctional organometallic reagents that allow the direct conversion of a broad range of carboxylic acid esters.[16] Recently, Nicewicz and co-workers designed an efficient synthesis of acridinium photocatalysts starting from xanthylium salts.[17]

Christof Sparr

Christof Sparr received his PhD from the ETH Zurich (Switzerland) working in the group of Prof. Ryan Gilmour. He then joined the groups of Prof. Dieter Seebach (ETH Zurich) and subsequently Prof. Steven V. Ley (University of Cambridge, UK). In 2013, Christof became habilitand mentored by Prof. Karl Gademann and since 2016, Christof has worked as Assistant Professor at the University of Basel. He is the recipient of the ETH silver medal, an SNSF starting grant, the Werner Prize of the Swiss Chemical Society 2017 and the Ruzicka Prize of the ETH Zurich 2018.

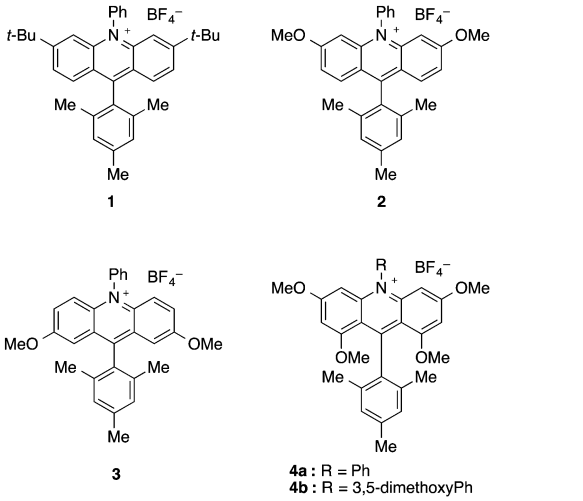

Scheme 2 Representative photocatalysts reported by Nicewicz and co-workers.

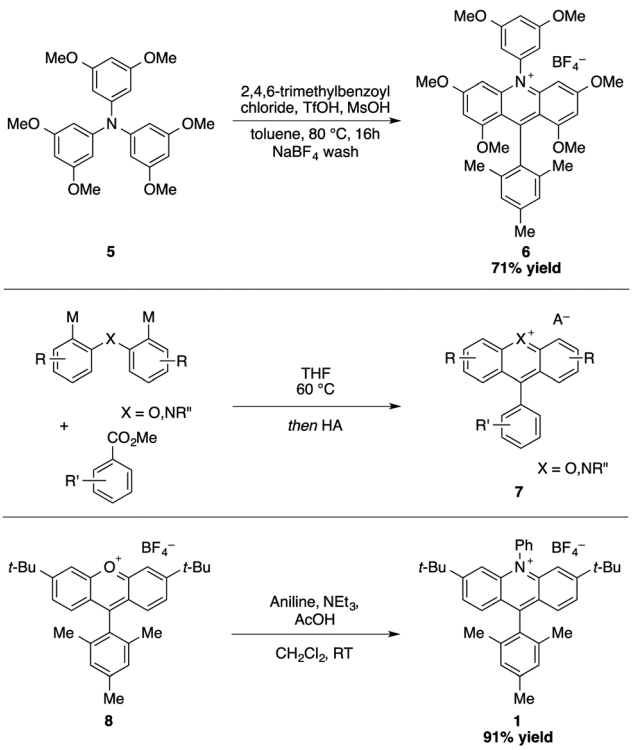

Scheme 3 Selected synthetic strategies for acridinium salts.

The rapid assembly of a xanthylium dye was thereby combined with a condensation reaction with an aniline to give the corresponding acridinium salt **1**.

Furthermore, an elegant strategy consisting of an oxidative Ugi-type reaction for the synthesis of a novel class of imide-acridinium salts has been developed by Mancheño and Alemán (Scheme 4).[18] Starting from *N*-substituted acridanes, a copper-catalysed oxidation takes place at the C9 position to give a cationic intermediate that reacts with the isocyanide. After addition of the *in situ* formed benzoate, the intermediate is

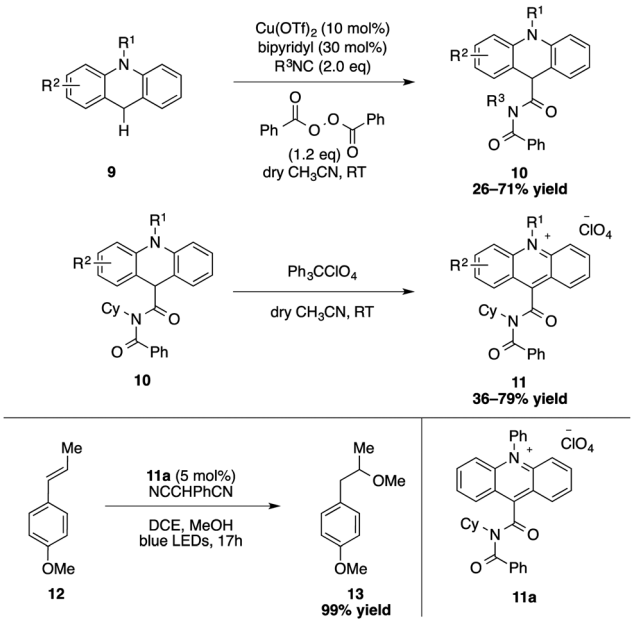

Scheme 4 Ugi reaction for the synthesis of acridinium photocatalysts and their application.

concomitantly rearranged in an Ugi-type fashion to produce the C9-substituted imide-acridanes **10**. A subsequent aromatization by hydride abstraction carried out by tritylperchlorate delivered the desired acridinium salt **11**. Photophysical and photoredox studies of these catalysts have been conducted.[19] Direct applications in photoredox catalysis were subsequently demonstrated with a suitable activity in several benchmarking transformation including *anti*-Markovnikov hydrofunctionalization of alkenes and a dehydrogenative lactonization.

3. Applications in photoredox chemistry

A rapidly growing number of chemical transformations employs acridinium salts as catalysts.[20–23] Photooxidations, polar radical crossover cycloaddition reactions, C–H functionalization, cross-coupling and cross-dehydrogenative reactions, are merely selected recent examples of the use of acridinium salts in photoredox catalysis.[24–30] A recent example from the Nicewicz group emphasises their unique features by the radical conjugate addition of *N*-carbamate-protected secondary amines (Scheme 5).[22] Notably, the reduction potential required for the formation of the α-radical is too high for common Ru- or Ir- based photocatalysts (*N*-Boc-piperidine, E_{ox} = 1.96 V *vs.* SCE). The application of strong excited-state oxidants such as the 9-mesityl-3,6-di-*t*-butyl-10-phenylacridinium salt or the Fukuzumi catalyst is hence required. This afforded the α-aminoalkylation of various carbamate protected secondary amines, including the substrate-controlled stereoselective synthesis of the natural product (+)-monomorine **15**.

Moreover, an acyl radical generation for the synthesis of asymmetric ketones was described by Fagnoni and co-workers (Scheme 6).[31] Starting from readily prepared acylsilanes, the oxidation to the corresponding radical cation by Fukuzumi's catalyst led to the aliphatic acyl radical after loss of the TMS group. The addition to a Michael acceptor followed by reduction and protonation delivered a variety of asymmetric ketones.

Recently, Glorius and co-workers disclosed a carbonyl olefin cross-metathesis catalysed by an acridinium salt derived from Nicewicz's 3,6-di-*tert*-butyl acridinium catalyst (Scheme 7).[32] 1,3-Diols are thereby generated from aldehydes **20** and alkenes **19** upon visible-light irradiation that subsequently undergo acid-promoted Grob-type fragmentations. After the elimination of acetone, the cross-metathesis product is thereby formed.

Using a cascade of C–H and C–C bond cleavage steps, the group of Leonori achieved an intriguing remote functionalization of nitriles and ketones induced by the photoexcited Mes-Acr-Me$^+$ catalyst (Scheme 8).[33] The key step of this transformation lies in the formation of an iminyl radical arising from the SET oxidation and deprotonation of a carboxylic acid containing cyclic oxime **22**. For instance, a stepwise sequence of an abnormal Beckmann fragmentation and a fluorination gives access to a broad range of distal fluorinated nitriles. This strategy could also be applied to the synthesis of γ-fluorinated and chlorinated ketones. After SET oxidation of a linear oxime **24**, a 1,5-hydrogen abstraction provides

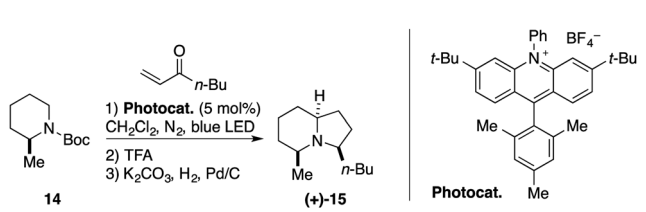

Scheme 5 Acridinium photocatalyzed α-alkylation of carbamate-protected secondary amines demonstrated by the synthesis of (+)-monomorine (**15**).

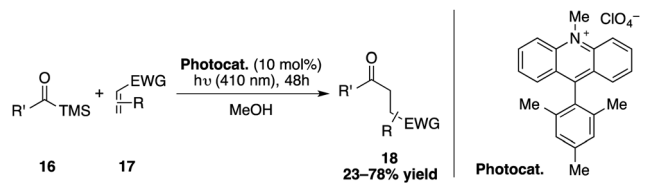

Scheme 6 Photocatalytic acylation of Michael acceptors.

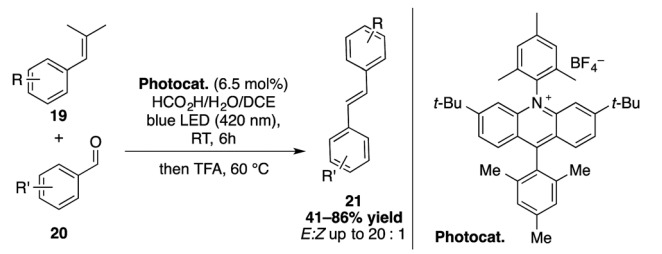

Scheme 7 Carbonyl olefin cross-metathesis for the synthesis of disubstituted *trans* alkenes.

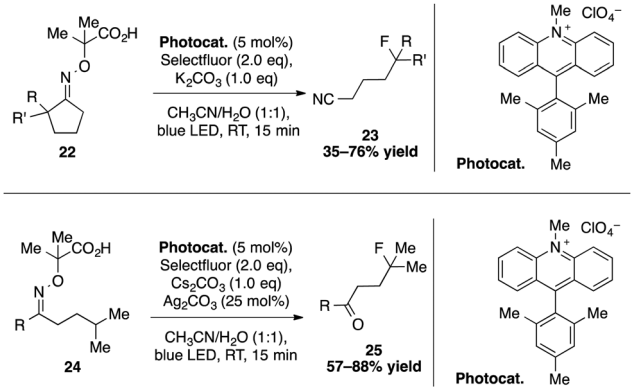

Scheme 8 Remote fluorination and chlorination *via* iminyl radicals.

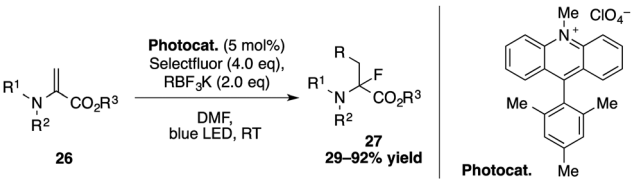

Scheme 9 Photocatalyzed synthesis of α-fluoro-α-amino acids.

a nucleophilic γ-radical that reacts with *N*-chlorosuccinimide or selectfluor to deliver the targeted compounds.

A photocatalyzed three-component carbofluorination for the synthesis of α-fluoro-α-amino acid derivatives has been developed by Molander and co-workers (Scheme 9).[34] Upon irradiation of the Mes-Acr-Me$^+$ catalyst, an alkyltrifluoroborate reagent is oxidized to give an alkyl radical that adds to the dehydroalanine to generate an α-amino radical intermediate, which reacts with selectfluor to provide the α-fluoro-α-amino acids **27**.

The Nicewicz group furthermore investigated an organophotoredox catalysed C–H fluorination of arenes with ^{18}F (Scheme 10).[35] Using the 9-mesityl-3,6-di-*t*-butyl-10-phenylacridinium salt as a photooxidant, TEMPO as a redox co-mediator and caesium fluoride combined with tetrabutylammonium bisulfate to generate TBAF *in situ*, the ^{18}F-fluorination of a wide range of arenes, heterocycles and even bioactive compounds was enabled. Their approach was expanded to radiofluorinations for PET imaging applications in diagnosis and pharmacological studies.

Several direct photoredox catalysed C(sp^2)–H functionalization reactions induced by a dual catalytic cobalt/Mes-Acr-Me$^+$ combination were explored by the group of Lei.[36,37] Among them an oxidative phosphonylation of arenes for the synthesis of valuable molecular scaffold is described (Scheme 11).[38]

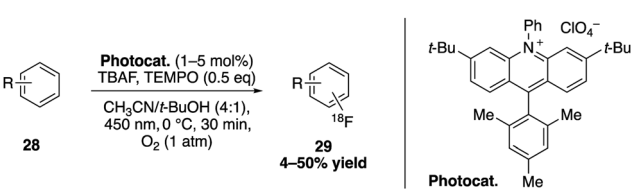

Scheme 10 Direct ^{18}F-fluorination catalysed by acridinium salts.

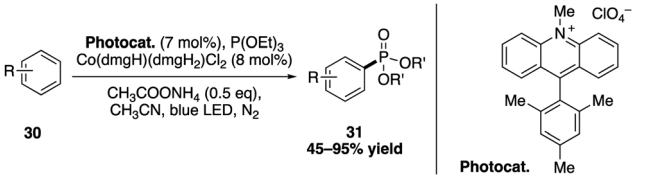

Scheme 11 Photooxidative phosphonylation of arenes.

The key step of this reaction is the SET oxidation of the arene to give a radical cation that reacts with the trialkylated phosphite. The resulting intermediate is then oxidized to a cationic intermediate which is subsequently deprotonated. By loss of an alkyl moiety, a wide range of aryl phosphonate products were obtained, even allowing the late stage functionalization of druglike compounds.

Extending the application of their dual catalytic cobalt/acridinium salt process, the same group also performed a photooxidative [4+2] annulation between aromatic ketimine derivatives and styrenes (Scheme 12).[39,40] The SET oxidation of the alkene substrate by the excited Mes-Acr-Me$^+$ catalyst thereby produces a radical cation that reacts with the nucleophilic aromatic ketimine to give a stable benzylic radical intermediate. A subsequent sequence consisting of a cyclization, oxidation and deprotonation allows to obtain highly substituted 3,4-dihydroisoquinolines with excellent *trans* diastereoselectivity.

The group of Kanai investigated a different type of dual catalytic palladium/acridinium systems for the catalytic dehydrogenation of N-heterocycles under visible light irradiation at ambient temperature (Scheme 13).[41] For tetrahydronaphthalenes, a thiophosphoric imide organocatalyst was added as a third component, allowing in this catalytic process the formation of hydrogen gas under mild conditions.

Exploiting the properties of the Mes-Acr-Me$^+$, Rueping and co-workers reported a cross-coupling of allylic C(sp^3)–H bonds with aryl- and vinylbromides, using a combination of nickel and an acridinium photocatalyst (Scheme 14).[16,42] After the oxidative addition of aryl- or vinylbromide to the nickel, a triplet–triplet energy transfer was proposed to take place between the excited acridinium salt and the nickel species. Cleavage of the halogen-metal-bond then generates the radical bromide, which abstracts a hydrogen from the alkene to form an allylic radical compound. The reaction with the Ni intermediate then undergoes a reductive elimination to release the allylarene **39** or corresponding 1,4-dienes.

Acridinium salts are not limited to visible light-induced catalysis but can also be used as organocatalyst based on their ground state redox properties. Taking advantage of those properties,

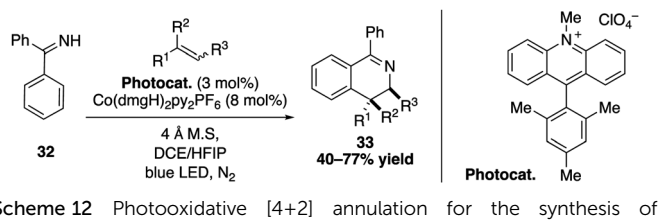

Scheme 12 Photooxidative [4+2] annulation for the synthesis of 3,4-dihydroisoquinolines derivatives.

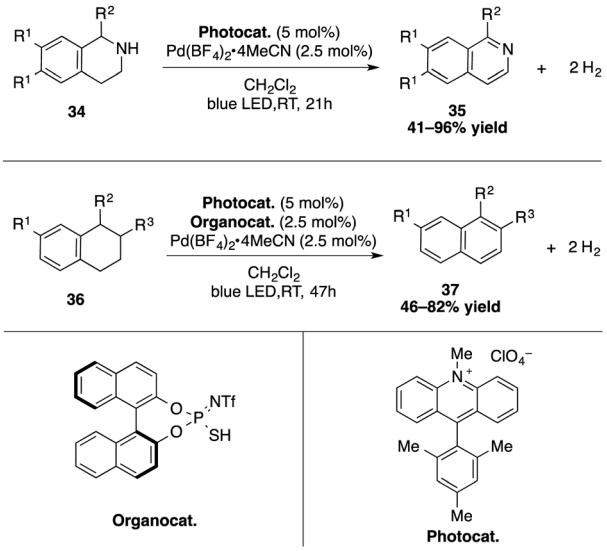

Scheme 13 Catalytic dehydrogenation of N-heterocycles and tetrahydronaphthalene derivatives.

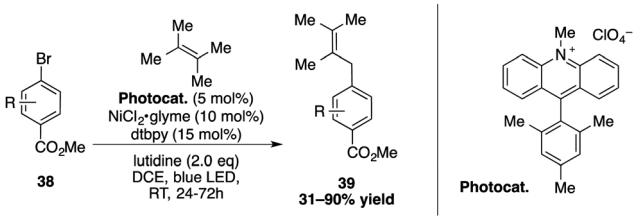

Scheme 14 Nickel dual catalytic cross-coupling for allylic arylation.

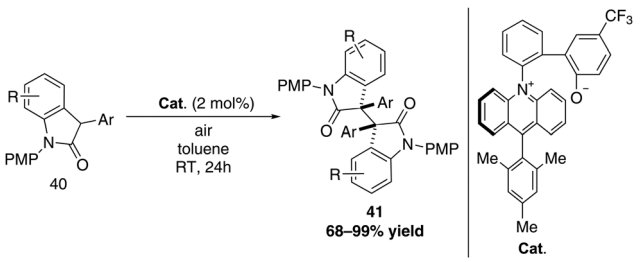

Scheme 15 Dimerization of 3-aryl oxindoles catalysed by an acridinium betaine.

Ooi and co-workers designed an interesting acridinium betaine catalyst that enables PCET (proton-coupled electron transfer) and applied it to the oxidative dimerization of oxindoles under air (Scheme 15).[43] The 9-mesityl acridinium moiety acts as the redox active unit whereas the phenoxide represents the substrate activation site. Using this catalyst, a successful homodimerization of 3-aryl oxindoles could be achieved.

4. Modulation of aminoacridinium photocatalysts

The evolution of the synthesis of acridinium salts towards more modular approaches allowed the diversification of their scaffold in order to tune their photophysical properties. To further modulate this class of catalysts, the authors aimed at the efficient synthetic preparation of aminoacridinium salts, which allow the lowering of the redox potential of the Fukuzumi catalyst ($E_{1/2}$ [P^*/P^-] = +2.06 V *vs.* SCE) up to the range of the Ir-based photocatalyst Ir[dF(CF$_3$)ppy]$_2$(dtbbpy)PF$_6$ ($E_{1/2}$ [P^*/P^-] = +1.21 V *vs.* SCE, Table 1).[16] With 1,8-substituted and asymmetric acridinium salts, a wide range of excited state reduction potential ranging from +1.19 V to +1.88 V against SCE was reached.[44,45] Also acridinium salts without amino functionalities were accessible, providing very high excited state reduction potentials of up to +2.32 V against SCE.[46] The excited state lifetimes of the photocatalysts are typically in the order of nanoseconds which render them suitable for photoredox catalysis.

5. Modular synthesis of acridinium salts

In order to access this range of acridinium salts, individual strategies were employed for a modular synthetic preparation. For the synthesis of symmetrically or unsubstituted acridinium salts, such as diamino derivatives, a 1,5-bifunctional organomagnesium reagent was added to a variety of carboxylic acid esters to provide a broad range of acridinium derivatives, some of which were scaled up to five grams (Scheme 16).[16,46]

The synthesis of 1,8-dimethoxy substituted acridinium dyes was achieved through a double directed *ortho*-metalation (D*o*M) to generate the 1,5-organodilithium reagent that was engaged in a direct ester to heterocycle transformation with variation of the carboxylic acid esters (Scheme 17).

This approach also enabled the synthesis of atropisomeric acridinium salts with a 1,8-dimethoxy-*peri*-substitution and 9-naphthyl moiety (**72**, Scheme 18).[46] After reduction of the racemic acridinium, the enantiomers of the *leuco*-form with a diastereomeric ratio of 97 : 3 were separated by HPLC and reoxidized by chloranil to give the two atropisomerically pure compounds. These compounds display a remarkable configurational stability with bond-rotational barriers of $\Delta G^{\ddagger}_{298K}$ = 124 kJ mol^{-1} and $\Delta G^{\ddagger}_{298K}$ = 127 kJ mol^{-1} respectively.

An entirely modular synthetic strategy for asymmetric acridinium salts was envisaged based on a combination of directed *ortho*-metalation (D*o*M) and halogen metal exchange (X–M) processes (Scheme 19). With this strategy, a broad panel of acridinium salts was obtained with various substitution patterns.[45]

6. Catalytic performance

The performances of these photocatalysts was verified in several benchmarking reactions. A photoredox/nickel dual catalytic decarboxylative cross coupling of Boc-L-proline (**75**) with methyl 4-iodobenzoate (**76**), originally reported by Doyle and MacMillan with an iridium photocatalyst, was the starting point of our inquiry.[47] The C–C coupling product **77** was obtained in very good yield (86%) using the mesityl-substituted diaminoacridinium catalyst **47** (Scheme 20).

Table 1 Photophysical and electrochemical properties of acridinium dyes

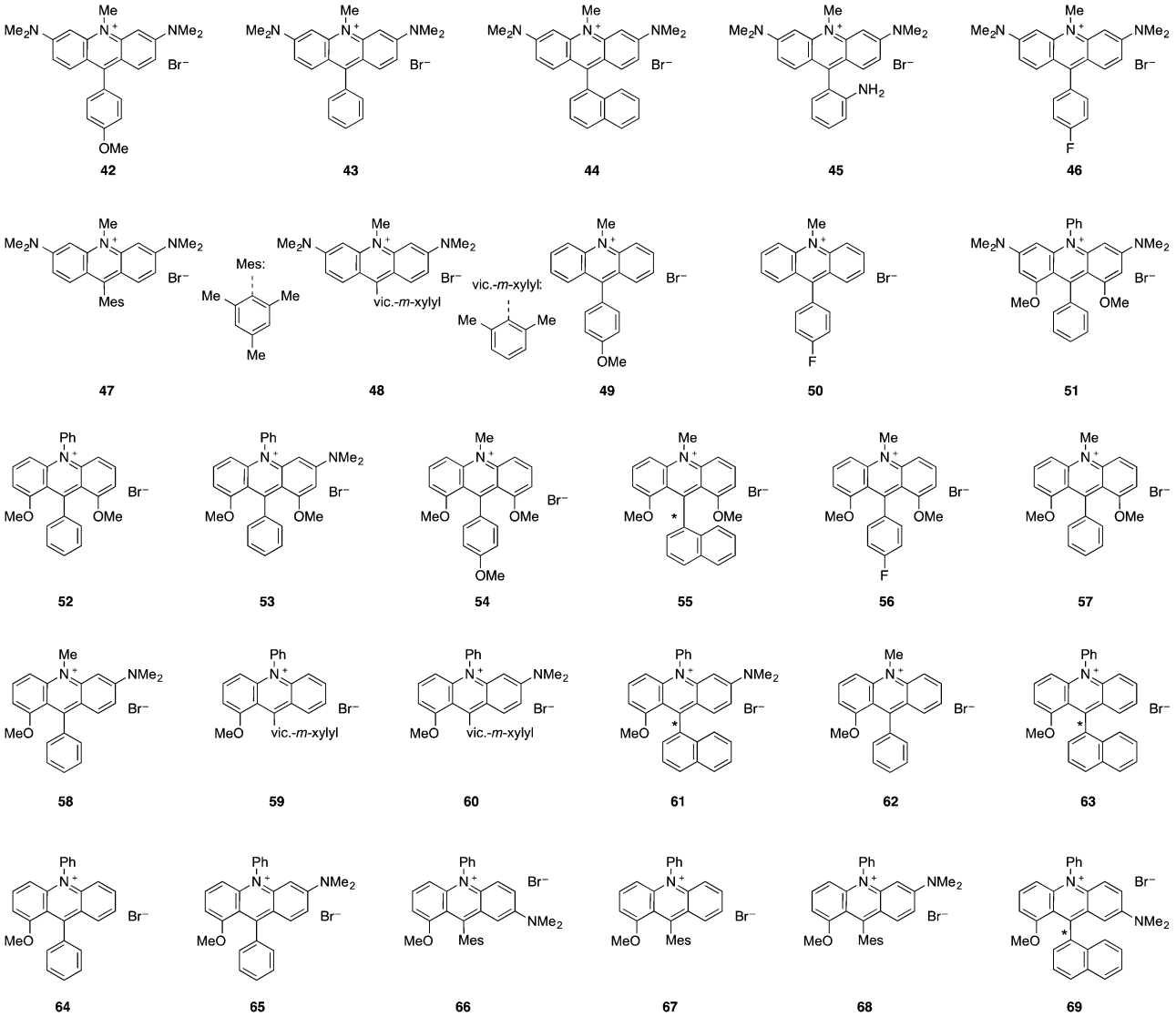

Dye	$\lambda_{abs,max}$ [nm]	$\lambda_{em,max}$ [nm]	$E_{0,0}$ [eV]	$E_{1/2}(P/P^-)$ [V]	$E_{1/2}(P^*/P^-)$ [V]	τ [ns]	HOMO–LUMO transition
Fukuzumi catalyst	425	—	2.57	−0.57	+2.08	6	CT
1	420	517	—	0.59	+2.08	14.4	—
2	407	525	—	−0.71	+2.01	3.0	—
3	466	545	—	−0.57	+1.90	18.7	—
4a	412	550	—	−0.84	+1.62	1.3, 8.9	—
4b	414	550	—	−0.82	+1.65	1.3, 12.3	—
42	501	531	2.41	−1.15	+1.26	—	—
43	502	534	2.40	−1.10	+1.30	—	—
44	506	534	2.39	−1.13	+1.26	—	—
45	506	532	2.39	−1.14	+1.25	—	—
46	503	534	2.40	−1.12	+1.28	—	—
47	503	534	2.40	−1.15	+1.25	2.2	π–π*
48	504	533	2.40	−1.15	+1.25	—	—
49	438	499	2.77	−0.56	+2.21	—	—
50	426	512	2.83	−0.51	+2.32	—	—
51	498	540	2.40	−1.19	+1.21	4.4	—
52	503	595	2.23	−0.47	+1.76	3.1	—
53	501	584	2.25	−0.94	+1.31	4.7	—
54	494	567	2.30	−0.62	+1.68	5.9	—
55	497	531	2.39	−0.51	+1.88	4.1	—
56	497	579	2.31	−0.51	+1.80	3.0	—
57	497	576	2.33	−0.52	+1.81	2.7	—
58	506	575	2.30	−0.83	+1.47	0.9, 4.4	π–π*

Table 1 (*continued*)

Dye	$\lambda_{abs,max}$ [nm]	$\lambda_{em,max}$ [nm]	$E_{0,0}$ [eV]	$E_{1/2}(P/P^-)$ [V]	$E_{1/2}(P^*/P^-)$ [V]	τ [ns]	HOMO–LUMO transition
59	480	634	2.25	−0.56	+1.69	1.2, 3.3, 16.8	Mixed
60	514	574	2.29	−0.90	+1.39	1.1, 7.2	π–π*
61	516	578	2.27	−0.87	+1.40	1.0, 6.2	Mixed
62	473	635	2.29	−0.48	+1.81	1.0, 3.0, 17.3	π–π*
63	480	635	2.26	−0.53	+1.73	1.0, 4.5	CT
64	479	637	2.23	−0.54	+1.69	1.0, 9.9	π–π*
65	511	576	2.29	−0.89	+1.40	1.0, 6.9	π–π*
66	583	723	1.94	−0.71	+1.23	1.5, 5.3	π–π*
67	479	632	2.25	−0.57	+1.68	1.4, 12.1	Mixed
68	513	573	2.29	−0.89	+1.40	1.1, 6.8	π–π*
69	590	755	1.87	−0.68	+1.19	0.9, 5.0	π–π*

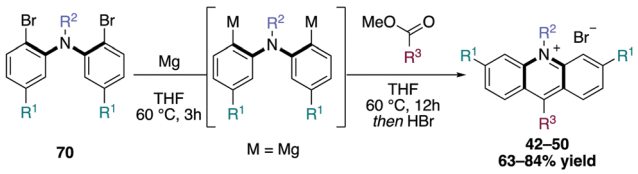

Scheme 16 1,5-bifunctional organomagnesium reagent for the synthesis of unfunctionalized and diamino acridinium dyes.

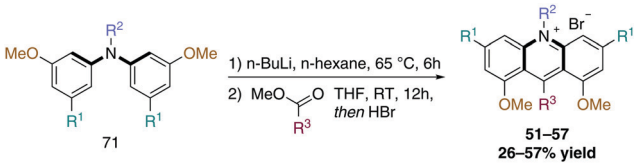

Scheme 17 Double directed *ortho*-metalation (dDoM) for the synthesis of 1,8-dimethoxy substituted acridinium salts.

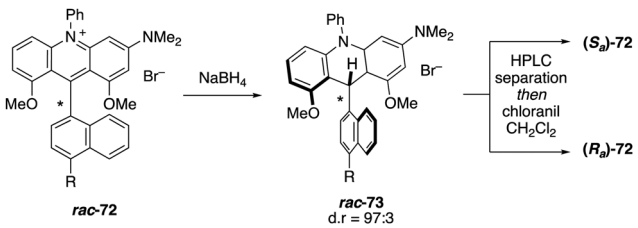

Scheme 18 Synthesis of atropisomeric acridinium salts.

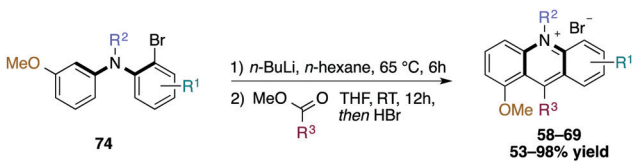

Scheme 19 Modular synthesis of asymmetric acridinium salts.

A comparative decarboxylative fluorination under the conditions described by MacMillan was then explored, revealing the ability of acridinium salts to complement polypyridyl transition metal systems and the organic 4-CzIPN photocatalyst (**78** to **79**, Scheme 21).[48] Originally catalysed by a ruthenium complex in the seminal report by Yoon, the [3+2]-cycloaddition

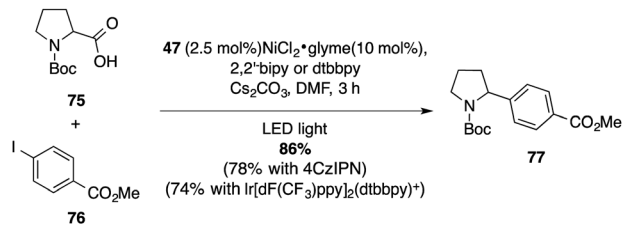

Scheme 20 Photoredox/Ni dual decarboxylative cross-coupling.

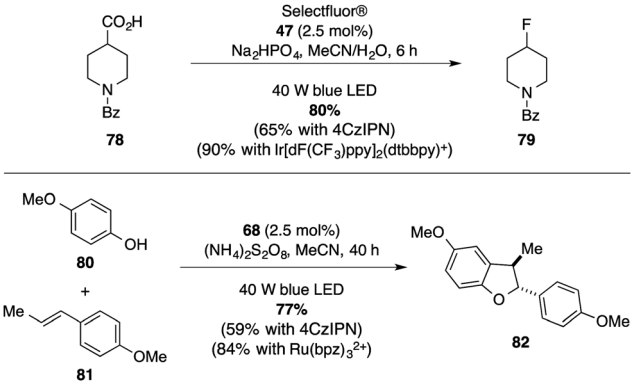

Scheme 21 Benchmark reactions.

providing dihydrobenzofuran **82** further confirmed the value of the acridinium catalyst library.[49]

Another validation of the utility of the modular acridinium salt assembly was obtained by the photodeuteration of clomipramine, developed by the MacMillan group.[50] Interestingly, a high selectivity for aliphatic positions was achieved with an average of 4 deuterium atoms per molecule, using a relatively low catalyst loading (1 mol%, Scheme 22).

The range of redox properties obtained by modulating the structure of aminoacridinium catalysts hence allows to employ

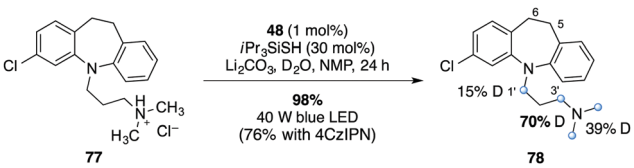

Scheme 22 Deuteration of clomipramine catalysed by an acridinium salt.

a common structural motif for a great variety of visible-light photoredox catalysed processes. Interestingly, a surprisingly high inherent photostability was found for the aminoacridinium salts. This property is likely required to design photocatalytic procedures while in other cases, tracing the fate of the photocatalyst during catalysis is expected to reveal interesting activation paths of utilized catalysts before a closed, productive cycle is entered. Besides the redox properties and stabilities, the kinetics, life time and energy of the excited states are other key parameters essential to refine photocatalytic reactions.

7. Conclusions

In recent years, a growing library of acridinium catalysts has been developed and utilized for various visible-light photocatalytic processes. This allowed tuning of the redox properties to a most suitable range for preparative photosynthetic applications. Similar to the polypyridyl transition-metal catalysts, amino substituents tend to lower the $E_{1/2}(P^*/P^-)$ by approximately 0.3–0.4 V while OMe groups typically allow fine tuning of the properties by 0.1–0.2 V. Moreover, alteration of substitution patterns also strongly influences the redox behaviour and thus allows further modification. Considering the numerous parameters contributing to the efficiency of the photocatalytic processes and their simultaneous variation during optimisation, it appears beneficial to employ catalysts of a common structural class to more rationally develop and improve the catalytic performance.

Conflicts of interest

The authors declare no conflict of interest. Some of the described acridinium and aminoacridinium catalysts are part of a filed patent (C. Fischer, C. Sparr. WO2019057451) licenced to Solvias. The aminoacridinium catalysts will soon be commercially available.

Acknowledgements

We gratefully acknowledge the Swiss National Science Foundation (BSSGI0-155902/1 and 175746), the University of Basel and the NCCR Molecular Systems Engineering for financial support. We thank Prof. M. Mayor for equipment usage, Prof. O. Wenger and Dr C. Kerzig for fruitful discussions, and Thomas Buchholz and Dragan Miladinov for skilful experimental support.

Notes and references

1 C. K. Prier, D. A. Rankic and D. W. C. MacMillan, *Chem. Rev.*, 2013, **113**, 5322–5363.
2 C.-S. Wang, P. H. Dixneuf and J.-F. Soulé, *Chem. Rev.*, 2018, **118**, 7532–7585.
3 K. N. Lee and M. Y. Ngai, *Chem. Commun.*, 2017, **53**, 13093–13112.
4 J. Twilton, C. C. Le, P. Zhang, M. H. Shaw, R. W. Evans and D. W. C. MacMillan, *Nat. Rev. Chem.*, 2017, **1**, 0052.
5 N. A. Romero and D. A. Nicewicz, *Chem. Rev.*, 2016, **116**, 10075–10166.
6 S. Fukuzumi and K. Ohkubo, *Org. Biomol. Chem.*, 2014, **12**, 6059–6071.
7 D. P. Hari and B. König, *Chem. Commun.*, 2014, **50**, 6688–6699.
8 S. Fukuzumi, H. Kotani, K. Ohkubo, S. Ogo, N. V. Tkachenko and H. Lemmetyinen, *J. Am. Chem. Soc.*, 2004, **126**, 1600–1601.
9 K. Ohkubo, K. Mizushima, R. Iwata, K. Souma, N. Suzuki and S. Fukuzumi, *Chem. Commun.*, 2010, **46**, 601–603.
10 M. Brasholz, *Acridinium Dyes and Quinones in Photocatalysis in Science of Synthesis, 'Photocatalysis in Organic Synthesis'*, 2018.
11 S. Fukuzumi, K. Ohkubo and T. Suenobu, *Acc. Chem. Res.*, 2014, **47**, 1455–1464.
12 T. Tsudaka, H. Kotani, K. Ohkubo, T. Nakagawa, N. V. Tkachenko, H. Lemmetyinen and S. Fukuzumi, *Chem. – Eur. J.*, 2017, **23**, 1306–1317.
13 S. Fukuzumi, K. Doi, A. Itoh, T. Suenobu, K. Ohkubo, Y. Yamada and K. D. Karlin, *Proc. Natl. Acad. Sci. U. S. A.*, 2012, **109**, 15572–15577.
14 M. Hoshino, H. Uekusa, A. Tomita, S. Y. Koshihara, T. Sato, S. Nozawa, S. I. Adachi, K. Ohkubo, H. Kotani and S. Fukuzumi, *J. Am. Chem. Soc.*, 2012, **134**, 4569–4572.
15 A. Joshi-Pangu, F. Lévesque, H. G. Roth, S. F. Oliver, L. C. Campeau, D. Nicewicz and D. A. DiRocco, *J. Org. Chem.*, 2016, **81**, 7244–7249.
16 C. Fischer and C. Sparr, *Angew. Chem., Int. Ed.*, 2018, **57**, 2436–2440.
17 A. R. White, L. Wang and D. A. Nicewicz, *Synlett*, 2019, 827–832.
18 A. Gini, M. Uygur, T. Rigotti, J. Alemán and O. García Mancheño, *Chem. – Eur. J.*, 2018, **24**, 12509–12514.
19 A. Gini, T. Rigotti, R. Pérez-Ruiz, M. Uygur, R. Mas-Ballesté, I. Corral, L. Martínez-Fernández, V. A. de la Peña O'Shea, O. García Mancheño and J. Alemán, *ChemPhotoChem*, 2019, 609–612.
20 F. Wu, L. Wang, J. Chen, D. A. Nicewicz and Y. Huang, *Angew. Chem., Int. Ed.*, 2018, **57**, 2174–2178.
21 L. Wang, F. Wu, J. Chen, D. A. Nicewicz and Y. Huang, *Angew. Chem., Int. Ed.*, 2017, **56**, 6896–6900.
22 J. B. McManus, N. P. R. Onuska and D. A. Nicewicz, *J. Am. Chem. Soc.*, 2018, **140**, 9056–9060.
23 K. A. Margrey, W. L. Czaplyski, D. A. Nicewicz and E. J. Alexanian, *J. Am. Chem. Soc.*, 2018, **140**, 4213–4217.
24 N. E. S. Tay and D. A. Nicewicz, *J. Am. Chem. Soc.*, 2017, **139**, 16100–16104.
25 J. B. McManus and D. A. Nicewicz, *J. Am. Chem. Soc.*, 2017, **139**, 2880–2883.
26 J. D. Griffin, C. L. Cavanaugh and D. A. Nicewicz, *Angew. Chem., Int. Ed.*, 2017, **56**, 2097–2100.
27 H. Liu, L. Ma, R. Zhou, X. Chen, W. Fang and J. Wu, *ACS Catal.*, 2018, **8**, 6224–6229.
28 K. C. Cartwright and J. A. Tunge, *ACS Catal.*, 2018, **8**, 11801–11806.
29 H. Cao, H. Jiang, H. Feng, J. M. C. Kwan, X. Liu and J. Wu, *J. Am. Chem. Soc.*, 2018, **140**, 16360–16367.
30 J. Davies, N. S. Sheikh and D. Leonori, *Angew. Chem., Int. Ed.*, 2017, **56**, 13361–13365.
31 L. Capaldo, R. Riccardi, D. Ravelli and M. Fagnoni, *ACS Catal.*, 2018, **8**, 304–309.
32 L. Pitzer, F. Sandfort, F. Strieth-Kalthoff and F. Glorius, *Angew. Chem., Int. Ed.*, 2018, **57**, 16219–16223.
33 E. M. Dauncey, S. P. Morcillo, J. J. Douglas, N. S. Sheikh and D. Leonori, *Angew. Chem., Int. Ed.*, 2018, **57**, 744–748.
34 J. Sim, M. W. Campbell and G. A. Molander, *ACS Catal.*, 2019, **9**, 1558–1563.
35 W. Chen, Z. Huang, N. E. S. Tay, B. Giglio, M. Wang, H. Wang, Z. Wu, D. A. Nicewicz and Z. Li, *Science*, 2019, **364**, 1170–1174.
36 G. Zhang, X. Hu, C. W. Chiang, H. Yi, P. Pei, A. K. Singh and A. Lei, *J. Am. Chem. Soc.*, 2016, **138**, 12037–12040.
37 G. Zhang, C. Liu, H. Yi, Q. Meng, C. Bian, H. Chen, J. X. Jian, L. Z. Wu and A. Lei, *J. Am. Chem. Soc.*, 2015, **137**, 9273–9280.
38 L. Niu, J. Liu, H. Yi, S. Wang, X. A. Liang, A. K. Singh, C. W. Chiang and A. Lei, *ACS Catal.*, 2017, **7**, 7412–7416.
39 X. Hu, G. Zhang, F. Bu and A. Lei, *Angew. Chem., Int. Ed.*, 2018, **57**, 1286–1290.
40 G. Zhang, Y. Lin, X. Luo, X. Hu, C. Chen and A. Lei, *Nat. Commun.*, 2018, **9**, 1225.
41 S. Kato, Y. Saga, M. Kojima, H. Fuse, S. Matsunaga, A. Fukatsu, M. Kondo, S. Masaoka and M. Kanai, *J. Am. Chem. Soc.*, 2017, **139**, 2204–2207.
42 L. Huang and M. Rueping, *Angew. Chem., Int. Ed.*, 2018, **57**, 10333–10337.
43 D. Uraguchi, M. Torii and T. Ooi, *ACS Catal.*, 2017, **7**, 2765–2769.
44 C. Fischer and C. Sparr, *Tetrahedron*, 2018, **74**, 5486–5493.

45 C. Fischer, C. Kerzig, B. Zilate, O. S. Wenger and C. Sparr, *ACS Catal.*, 2020, **10**, 210–215.
46 B. Zilate, C. Fischer, L. Schneider and C. Sparr, *Synthesis*, 2019, 4359–4365.
47 Z. Zuo, D. T. Ahneman, L. Chu, J. A. Terrett, A. G. Doyle and D. W. C. MacMillan, *Science*, 2014, **345**, 437–440.
48 S. Ventre, F. R. Petronijevic and D. W. C. Macmillan, *J. Am. Chem. Soc.*, 2015, **137**, 5654–5657.
49 T. R. Blum, Y. Zhu, S. A. Nordeen and T. P. Yoon, *Angew. Chem., Int. Ed.*, 2014, **53**, 11056–11059.
50 Y. Y. Loh, K. Nagao, A. J. Hoover, D. Hesk, N. R. Rivera, S. L. Colletti, I. W. Davies and D. W. C. Macmillan, *Science*, 2017, **1187**, 1182–1187.